JOURNAL OF GEOPHYSICAL RESEARCH, VOL. 101, NO. D11, PAGES 16,807–16,816, JULY 20, 1996

Effects of clouds and haze on UV-B radiation

Jeral G. Estupiñán[1] and Sethu Raman

Department of Marine, Earth and Atmospheric Sciences, North Carolina State University, Raleigh

Gennaro H. Crescenti[2] and John J. Streicher[2]

Atmospheric Sciences Modeling Division, Air Resources Laboratory, National Oceanic and Atmospheric Administration, Research Triangle Park, North Carolina

William F. Barnard

Atmospheric Processes Research Division, National Exposure Research Laboratory, U. S. Environmental Protection Agency, Research Triangle Park, North Carolina

Abstract. An experiment was conducted over a 6-month period in Research Triangle Park, North Carolina, to investigate the effects of clouds and haze on ultraviolet (UV) radiation. Data were collected using a Yankee Environmental Systems UVB-1 pyranometer, an Eppley Laboratory Precision Spectral Pyranometer, and a SCI-TEC Brewer spectrophotometer. Hourly reports of total cloud cover and surface observations of air temperature, dew point temperature, barometric pressure, and visibility from the National Weather Service located at the nearby Raleigh-Durham International Airport were also used in this study. An empirical relationship has been formulated for UV-B attenuation as a function of total solar transmissivity and cloud cover. Cumulus-type clouds were found to attenuate up to 99% of the incoming UV-B radiation during overcast conditions. However, these same clouds were found to produce localized increases of UV-B radiation of up to 27% over timescales less than 1 hour under partly cloudy skies when the direct solar beam was unobstructed. Summer haze was found to attenuate UV-B radiation in the range of 5% to 23% when compared to a clear day in the autumn. In general, total radiation was attenuated more than UV-B radiation under cloudy conditions.

Introduction

Ultraviolet (UV) radiation is divided into several categories: extreme UV (10–120 nm), far UV (120–200 nm), UV-C (200–280 nm), UV-B (280–315 nm), and UV-A (315–400 nm). While radiation associated with wavelengths shorter than 280 nm is extremely harmful to plants, animals, and humans, it almost never reaches the Earth's surface because of oxygen and ozone (O_3) absorption in the stratosphere. However, some of the radiation associated with the UV-B range does reach the Earth's surface and represents a potential hazard to many life forms [*Koller*, 1965; *Setlow*, 1974; *Peak et al.*, 1984; *Sullivan*, 1992]. The more generally accepted range in the practice of observing UV-B radiation is between 280 and 320 nm (due to the cutoff in ozone absorption).

An increase in awareness of the harmful effects of exposure to UV-B radiation has led the National Weather Service (NWS), in cooperation with the Environmental Protection Agency (EPA), to develop the UV Exposure Prediction Index (UVI) for wavelengths between 290 and 400 nm [*Miller et al.*, 1993]. This forecast is distributed daily to 58 cities in the United States to alert the public of the potential hazards to prolonged UV exposure. The UV Index is forecasted daily for the next day at local solar noon. However, the prediction index is based on some simple parameterizations. For example, aerosols and attenuating gases other than stratospheric O_3 are not included in the current algorithm. This study has been conducted in an attempt to examine how UV-B radiation is attenuated by clouds and haze. The information presented here may be used to better parameterize UV-B attenuation within the prediction index algorithms.

Some of the factors which contribute to UV-B attenuation for clear sky conditions are solar zenith angle, Earth-Sun distance, altitude above mean sea level, total column O_3 concentration, total column aerosol concentration, minor tropospheric constituents such as nitrogen dioxide (NO_2) and sulfur dioxide (SO_2), and UV surface albedo. Under cloudy conditions the interaction of UV-B radiation with the Earth's atmosphere is more complex. While clouds can decrease direct radiation, they can produce an increase in the amount of diffuse radiation reaching the Earth's surface. Factors such as cloud location, percent cover, cloud optical thickness, liquid water content, and particle distribution make it difficult to develop a quantitative relationship relating cloud properties to the attenuation of UV-B radiation. Unfortunately, very little is known about how these factors affect UV-B radiation.

Several studies have been conducted to quantify the attenuation of UV radiation by clouds. *Ilyas* [1987] showed that clouds reduced the clear sky UV radiation by a factor of

[1]Now at Department of Geography, University of Colorado at Boulder.

[2]On assignment to the National Exposure Research Laboratory, U. S. Environmental Protection Agency, Research Triangle Park, North Carolina.

Paper number 96JD01170.
0148-0227/96/96JD-01170$09.00

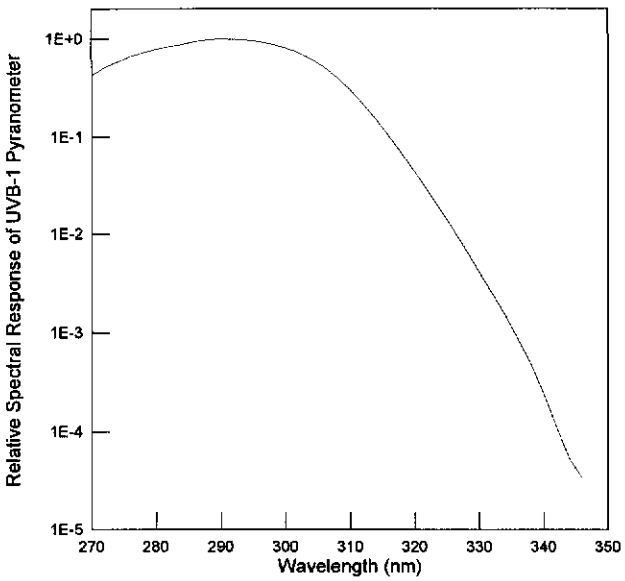

Figure 1. Spectral response of the Yankee Environmental Systems UVB-1 pyranometer.

$1-0.056CD$, where CD is the number of tenths of the sky that is covered by clouds. *Cutchis* [1980] and *Josefsson* [1986] derived reduction factors similar to that obtained by *Ilyas* [1987]. The former study showed that overcast conditions limited the incoming radiation by 50% in the United States while the later showed that the radiation was reduced by 70% in Sweden under similar conditions. *Bais et al.* [1993] established a relationship between the UV-B radiation and cloud cover in Greece when the solar zenith angle was 50° and cloud coverage was at least 25%. *Paltridge and Barton* [1978] derived an empirical function which relates erythemal dose as a function of cloud cover for Australia.

Very little research has been conducted in the southeastern United States investigating the attenuation of UV-B radiation by haze. *Miller et al.* [1993] compared UV-B measured values from spectrophotometers located in Research Triangle Park (RTP), North Carolina, and Toronto, Canada, against the predicted values of the Ultraviolet Potential Index (UVP) which does not include attenuation factors for clouds. They found that the summer UV-B values in RTP were considerably lower than the predicted UVP values while no significant differences were found for Toronto. *Miller et al.* [1993] suggest that this decrease in UV-B radiation found in RTP can be explained by the presence of tropospheric air pollution. *Justus and Murphey* [1994] also found that UV-B radiation decreased by 10% due to changes in aerosol concentrations in Atlanta, Georgia, from 1980 to 1984.

The objectives of this study are to establish an empirical relationship which describes the attenuation of UV-B radiation as a function of total solar transmissivity and cloud cover; to investigate the attenuation of UV-B by summer haze; to compare the attenuation by clouds and haze for UV-B wavelengths to that for total global radiation; and to study the effects of scattering by clouds which may increase local UV-B radiation.

Experimental Setup and Data

Data were collected over a 6-month period from June 14, 1994, to December 11, 1994. This time period was chosen to examine how UV-B radiation is affected by clouds on a seasonal timescale.

A Yankee Environmental Systems UVB-1 pyranometer was used to measure global UV-B irradiance between wavelengths of 280 and 320 nm. The manufacturer specified accuracy is 10% of observed measurement for solar zenith angles between 0° and 50°, 6% between 50° and 60°, and 8% between 60° and 70°. The specified cosine response is 5% for solar zenith angles between 0° and 60°. The response time of the sensor is 0.1 s. The instrument was calibrated by Yankee Environmental Systems prior to the start of the study. The spectral response of the instrument, shown in Figure 1, is very similar to the erythemal response.

An Eppley Laboratory Precision Spectral Pyranometer (PSP) was used to measure total global solar radiation between wavelengths of 285 and 2800 nm. The manufacturer specified cosine error of the instrument is 1% from solar zenith angles between 0° and 70° and 3% from zenith angles between 70° and 90°. The response time of the sensor is 1 s. The instrument was calibrated by Eppley Laboratory prior to the start of the study.

Both of these pyranometers were located at the southwestern corner on the roof of an EPA building in RTP (35° 54' N, 78° 53' W). The roof of the building is about 12 m above ground level. The two sensors were located side by side on top of a wooden platform approximately 1.5 m above the base of the roof. A portion of the building northeast of the two radiation sensors extends above the roof. However, that part of the building obstructed only 15° of view above the horizon between 30° and 60° azimuth. To the south, several trees partially obstructed about 20° of view from the horizon when they were in full foliage. Data from both of these pyranometers were acquired at 1 Hz and recorded as 5-min averages using a Campbell Scientific CR-10 data logger.

A SCI-TEC, Inc. Brewer spectrophotometer (model MKIV) which measures total column O_3, NO_2, SO_2, as well as surface UV-B radiation was used to measure total column O_3. The overall stability of the spectrophotometer (checked several times per day by an internal halogen lamp) was found to be better than 1.8% over a 2-year period. The spectral response of the instrument was checked once a week using several external UV lamps. The manufacturer specified accuracy for total column O_3 is 1%. The manufacturer specified accuracy for UV-B is 8% for wavelengths less than 300 nm and 4% for wavelengths greater than 300 nm. The cosine response decreases from unity at a zenith angle of 0° to 0.79 for a zenith angle of 85°.

The spectrophotometer was located on the top of a 12 m platform (35° 53' N, 78° 53' W) near the edge of a grass field. The area is clear of trees to a radius of 40 to 100 m. The sky is free from obstructions except from about 44° to 76° azimuth where pine trees block the field of view up to 5° above the horizon. A 30-m meteorological tower is located about 15 m southeast of the platform (138° azimuth). The spectrophotometer measured total column O_3, SO_2, and NO_2 at predetermined absorption wavelengths and recorded these data about 20 times per day on a personal computer. UV-B scans were manually obtained twice per day when the solar zenith angle was 38°.

Both sites are approximately 90 m above mean sea level and are separated by about 2 km. They are both approximately 10 km west of a NWS observation station (35° 52' N, 78° 47' W, 130 m above mean sea level) located at the Raleigh-Durham International Airport (RDU). Hourly reports of total cloud

Table 1. Coefficients for the Third-Degree Polynomial for Ideal Clear Sky Days of June 19 and September 19, 1994

Date	Solar Elevation	a_0	a_1	a_2	a_3
June 19	20° to 77°	0.565590	−0.0581388	0.00264938	-1.89372×10^{-5}
	77° to 20°	0.979913	−0.0869666	0.00336516	-2.42892×10^{-5}
September 19	20° to 56°	0.517012	−0.0586608	0.00294805	-2.13361×10^{-5}
	56° to 20°	0.703623	−0.0690292	0.00340665	-2.71528×10^{-5}

The equation gives ideal clear sky value of UV-B radiation I_c (W m^{-2}) as a function of solar elevation θ (degrees). $I_c = a_0 + a_1\theta + a_2\theta^2 + a_3\theta^3$

cover, and surface observations of air temperature, dew point temperature, barometric pressure, and visibility observed at this station were also used in this study. The overall albedo of the area is 0.15 [*Page*, 1980].

Methodology

UV-B attenuation α_B was calculated using the expression

$$\alpha_B = \frac{I_m - I_c}{I_c} \tag{1}$$

where I_m is the UV-B irradiance measured by the Yankee Environmental Systems UVB-1 pyranometer and I_c is the UV-B irradiance that would have been received at the Earth's surface under an ideal clear sky. Two days were selected (June 19 and September 19, 1994) to approximate an ideal clear sky in which no clouds were present during the daylight hours. June 19 and September 19 had visibilities which were typical of the summer and autumn, respectively. Idealized curves were determined for both days by fitting I_m as a function of solar elevation angle θ using a third-degree polynomial. The polynomial was broken up into morning and afternoon components for each day. The coefficients are listed in Table 1. Computed values of α_B for the summer months used the polynomial fit for June 19, while the September 19 curve was applied to the data collected in the autumn.

For relatively clear summer days when the total cloud cover was less than 20% over the entire day, α_B generally varied by no more than 10% from the June 19 idealized curve. For similar days in the autumn, the maximum variability was no more than 15% from the September 19 curve. The summer variability is mainly due to varying amounts of haze (i.e., higher humidity), while the autumn variability is probably due to more frequent changes in atmospheric synoptic weather patterns (i.e., varying air masses).

The UV-B attenuation was adjusted for variations in total column O_3 using a two-stream delta-Eddington radiative transfer model [*Madronich*, 1993]. Only O_3 absorption cross sections were used in the model [*Molina and Molina*, 1986]. Vertical profiles of O_3, temperature and barometric pressure were obtained from the U. S. Standard Atmosphere. Table 2 lists the average values over the daylight hours for surface O_3 and total column O_3, SO_2, and NO_2 for the two ideal clear sky days which were used in this model.

The total solar transmissivity T_s was calculated using

$$T_s = \frac{S_m}{S} \tag{2}$$

where S_m is the total solar radiation measured at the surface with the Eppley PSP and S is the total solar radiation reaching the top of the atmosphere which is defined as

$$S = S_o\left(\frac{d_o}{d}\right)^2 \cos\phi \tag{3}$$

where S_o is the solar constant (1367 W m^{-2}), d and d_o represent the actual and mean Earth-Sun distance, respectively, and ϕ is the solar zenith angle.

Since total solar attenuation α_S is more dependent on the water vapor effects than UV-B radiation, it was calculated using the relationship

$$\alpha_S = \frac{S_m}{S_c} \tag{4}$$

where S_c is the total global radiation that would reach the Earth's surface under clear sky conditions. A broadband radiation model was used to compute S_c [*Iqbal*, 1983]. The model gives the total broadband solar radiation in two components: direct plus diffuse. The diffuse irradiance includes contributions due to Rayleigh and aerosol scattering, as well as a downward irradiance due to multiple reflections between the ground and the atmosphere. This model requires surface air temperature, dew point, barometric pressure, visibility, and total column O_3 as input variables. The first four variables were obtained from the RDU NWS observations while the last was acquired by spectrophotometer measurements.

Data for solar zenith angles greater than 70° have not been used in this study to reduce possible contamination from sur-

Table 2. Daytime-averaged Surface O_3 and Total Column O_3, SO_2 and NO_2 Values for the Two Ideal Clear Sky Days of June 19 and September 19, 1994, Determined by the Brewer Spectrophotometer

Date	Surface O_3, ppbv	Total Column O_3, DU	Total Column SO_2, DU	Total Column NO_2, DU
June 19	30	314.9	5.4	0.49
September 19	20	292.9	3.0	0.54

DU is Dobson units.

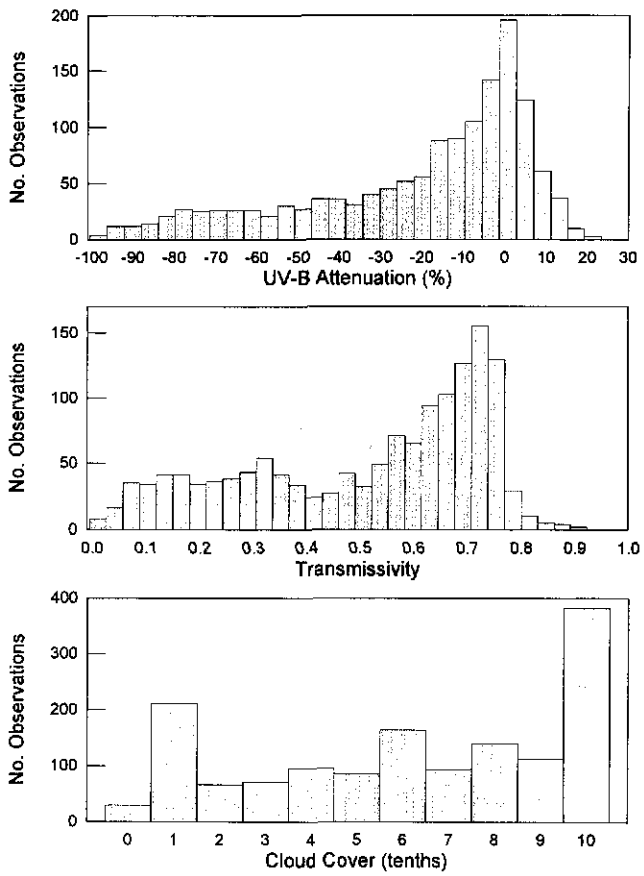

Figure 2. Histograms of UV-B attenuation, total solar transmissivity, and cloud cover from June 14, 1994, to December 11, 1994, for solar zenith angles less than 70°.

rounding obstacles. The equations used to calculate the position of the Sun were adopted from *Spencer* [1971] where the eccentricity correction for the Earth's orbit, the equation of time, and the declination are expressed in the form of Fourier series expansions.

Analysis and Results

UV-B Attenuation as a Function of Solar Transmissivity and Cloud Cover

Correlations between UV-B attenuation α_B with the atmospheric transmissivity T_s and cloud cover CD can be used for the prediction of UV-B radiation reaching the Earth's surface. A large negative correlation of -0.93 was found for α_B and T_s for the entire data set collected in this study. A moderate correlation of 0.60 was found for α_B and CD. Figure 2 shows the histograms of UV-B attenuation, total solar transmissivity, and cloud cover for the entire 6-month data set. Note there is a slight decrease in the number of observations when the T_s is between 0.4 and 0.5. *Liu and Jordan* [1960] show that when the transmissivity is 0.4, the diffuse radiation reaching the Earth's surface is maximum. The mechanism for creating these high diffusion values is due to scattering by altocumulus and altostratus clouds [*Haurwitz*, 1948]. It is possible that this decrease in observations when T_s is between 0.4 and 0.5 may be due to a lack of these cloud types during much of the study period as shown by the RDU data. It is also possible that a bimodal distribution might be expected under partly cloudy conditions since the solar disk may or may not be obstructed.

A least squares second-order polynomial was used to fit α_B as a function of T_s and CD. The derived relationship is

$$\alpha_B = a_0 + a_1 CD + a_2 T_s + a_3 CD^2 + a_4 T_s CD + a_5 T_s^2 \qquad (5)$$

where $a_0 = -70.4329$, $a_1 = -2.79165$, $a_2 = 171.6308$, $a_3 = 0.013657$, $a_4 = 3.805116$, and $a_5 = -102.629$. For example, when the $T_s = 0.5$ and $CD = 5$, then $\alpha_B = -14\%$. Figure 3 is a contour plot of α_B as a function of T_s and CD. The determination coefficient for this fit was 0.95 with a root mean square error of 8.5%. Similar results were found by *Bais et al.* [1993].

A difference of 1% was observed between predicted and measured UV-B attenuation for 22% of the data set. Differences of 10%, 15%, and 20% were found for 77%, 92%, and 97% of the data set, respectively. There was little variation between the predicted and measured values of α_B for low transmissivity and overcast conditions. Conversely, large differences were found between the predicted and measured values of α_B when the transmissivity was small and the sky was relatively clear. This is because there were very few instances when heavy hazes were accompanied by clear skies.

This relationship has the advantage that it uses the transmissivity of the atmosphere in the prediction of α_B in comparison with previous relationships found in the literature (Figure 4). Cloud types have not been considered since the same cloud type can attenuate different amounts of radiation due to variations in thickness, shape, or position [*Frederick and Steele*, 1995].

The relationship derived by *Bais et al.* [1993] predicts up to a 4% increase in UV radiation above the normal clear sky levels when cloud coverage is less than 40%. Equation 5 predicts increases in UV-B radiation above the normal clear sky levels when the amount of cloud cover increases. This is due to an increase in the local transmissivity due to reflection from clouds. When the direct beam is obstructed by thin clouds or fog, there is a decrease in the direct solar irradiance but an

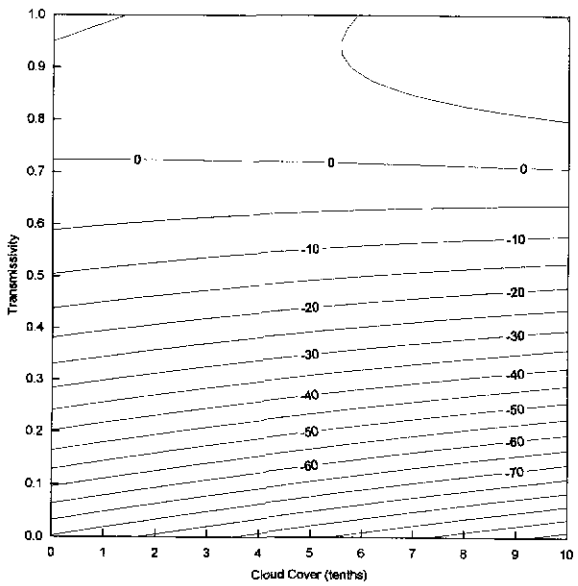

Figure 3. Contour plot of the least squares regression of UV-B attenuation (%) as a function of total solar transmissivity and cloud cover (tenths).

increase in the scattered radiation. The net result is a decrease in the total amount of radiation. Although probably rare, it is possible to find some enhancements even with complete overcast conditions.

There are some deficiencies in the relationship derived in this study. The maximum predicted UV-B radiation will be valid for near overcast conditions but not for a complete overcast since it is not possible to observe an increase in UV-B radiation greater than normal clear sky values when the sky is completely overcast. This is an artifact of the statistical fit for the UV flux corresponding to the spectral range of the UVB-1 pyranometer. Data acquired from other UV pyranometers may yield varying but similar results.

This relationship presents an improvement as a forecast tool to predict the effects of cloud cover to UV-B radiation. However, more work needs to be conducted on the development of a relationship that will include other factors affecting the UV-B attenuation such as cloud optical depth, cloud water, and cloud droplet size distribution.

Table 3. UV-B Attenuation α_B, Visibility, Dew Point Temperature, and Wind Speed for 12 Clear Summer Days Against the Clear Sky Day of September 19

Date	α_B, Percent	Visibility, km	Dew Point, °C	Wind Speed, m s^{-1}
June 15	−23	10	22.8	2.01
June 16	−23	10	22.2	2.10
June 19	−13	16	21.1	0.76
July 4	−18	24	22.2	2.41
July 9	−9	10	21.7	3.93
July 10	−10	19	21.7	3.17
July 14	−6	16	22.8	4.34
July 15	−12	11	24.4	3.71
July 16	−13	16	21.7	2.73
July 25	−22	6	22.8	3.22
August 6	−5	10	21.7	4.29
August 9	−17	24	16.7	1.25

UV-B attenuation was calculated when the solar zenith angle was 34° in the morning.

Summer Versus Autumn UV-B Radiation

The effects of haze on UV-B radiation were examined by comparing several clear sky summer days against the clear sky day of September 19. The selected summer days were subject to various amounts of haze while September 19 was relatively dry (dew point temperature of 10°C) and haze free (visibility of 32 km). Table 3 lists α_B, visibility, dew point temperature, and wind speed for these days when measurements were taken at a morning solar zenith angle of 34°. Figure 5 displays curves for these 12 days as solid lines compared to September 19 (dashed line). These data were acquired in the morning for solar zenith angles between 34° and 70°. Afternoon data were not used because of convective activity which produced numerous cumulus clouds. Data were also limited to the times when the solar zenith angle was greater than 34°, which is the minimum solar zenith angle observed on September 19. The effect of the variation in total column O_3 on UV-B radiation between September 19 and the twelve summer days was corrected using *Madronich*'s [1993] model. It is apparent from these curves that haze does have an attenuating effect on UV-B radiation, especially for low solar zenith angles. The average decrease for all 12 days was 12% when the solar zenith angle was smallest (~ 35°).

Negligible correlation coefficients of −0.11 and −0.03 were found between α_B and visibility and α_B and dew point, respectively, for the 12 days. A more moderate correlation coefficient of −0.60 was obtained for α_B and surface wind speed. Stronger winds are generally associated with a decrease in UV-B attenuation, which are probably due to cleaner air masses which follow the passage of cold fronts. However, no conclusion can be drawn from such a limited data set. Data should be collected over the course of several summer seasons, and preferably in several locations, before definite conclusions can be drawn about UV-B attenuation and its relationship to surface wind speed. A large data set such as this would also help determine if the correlation between α_B and surface wind speed are local or global in nature.

The UV-B radiation was examined for 31 relatively clear mornings using measurements when the solar zenith angle was 60°. The UV-B radiation increases from summer to autumn due to an increase in transmissivity and a decrease in total column O_3. Figure 6 shows this increase in UV-B radiation and transmissivity, as well as a decrease in total column O_3 after adjusting for the Earth-Sun distance. The figure shows that the UV-B radiation and transmissivity remain relatively constant during the summer when the solar zenith angle was 60°. The effects of haze on UV-B radiation dominate more during the summer than during the autumn. During the autumn, there is much less haze and its effect on the incoming UV-B radiation is weaker. Figure 7 shows the linear relationship between UV-B radiation and total column O_3. Future studies over a longer period of time should be conducted to investigate the effects of haze on UV radiation. The current UV Index will benefit from derived empirical relationships that could relate meteorological parameters such as visibility, surface dew point temperature, or precipitable water to the amount of UV radiation reaching the surface.

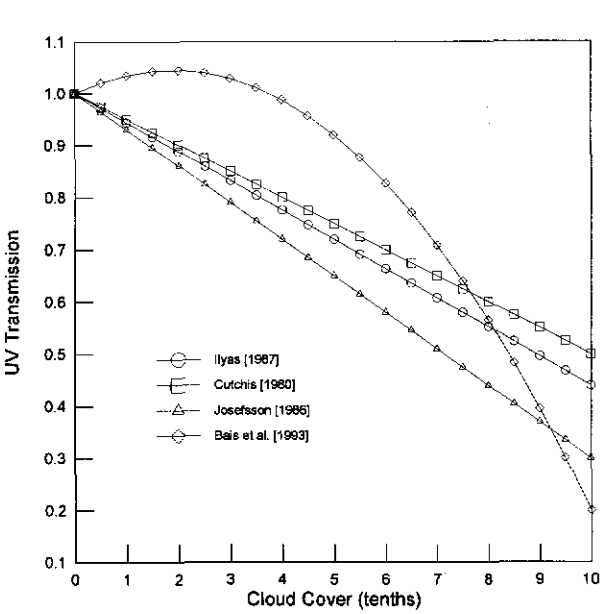

Figure 4. UV transmissions established from previous studies.

Attenuation of Total Solar and UV-B Radiation

The attenuation of total solar radiation α_S was calculated for the summer months and compared with the α_B for the same time period. The average dew point temperature and visibility

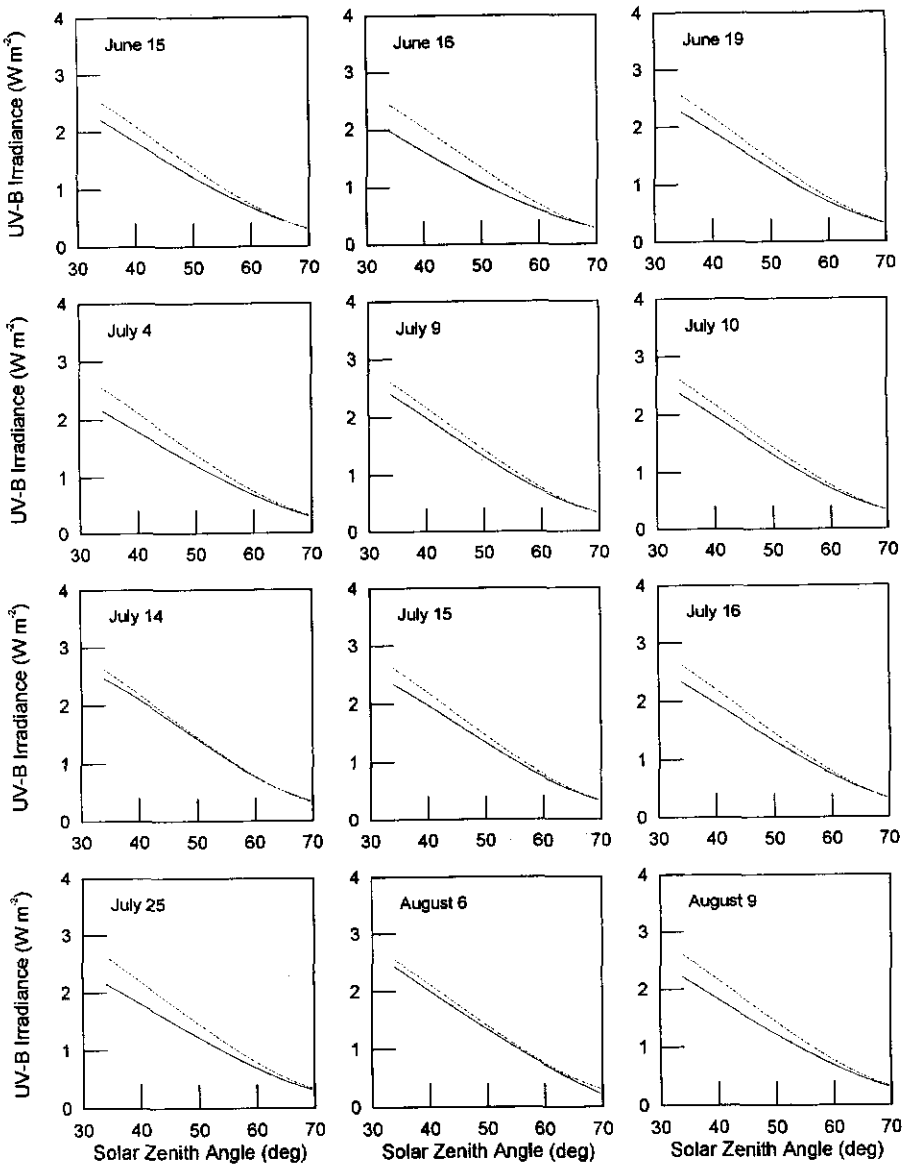

Figure 5. Difference in UV-B radiation between 12 summer days (solid line) and September 19 (dashed line). Note that the ozone correction was done by scaling the summer ozone values to that of June 19 and the autumn values to that of September 19.

for the summer were 20.5°C and 14.4 km, respectively. The variability in the magnitude of the predicted transmissivity was estimated using various solar elevations, visibilities (ranging from 10 to 24 km) and dew point temperature (ranging from 18 to 25°C). The difference in the predicted transmissivities was found to be less than 6% for average summer time conditions at RDU.

Blumthaler and Ambach [1988] found that total solar radiation was attenuated more effectively than UV-B radiation by a factor of 1.2 in the Swiss Alps. Similar results were found by *Dickerson et al.* [1982] in which clouds attenuated total radiation 20% more than UV radiation. However, *Frederick et al.* [1993] found that the total radiation attenuation was the same as UV-B attenuation. *Frederick et al.* [1993] explained that the difference between their study (conducted in Chicago) and the study conducted by *Blumthaler and Ambach* [1988] could have been caused by different chemicals dissolved within cloud droplets, which in turn, could have affected α_B. Total radiation was attenuated 24% more than UV-B radiation in our study. *Figure 8* shows the difference between total solar and UV-B attenuation ($\Delta\alpha = \alpha_S - \alpha_B$) as a function of the transmissivity T_s. In this case, the transmissivity was defined as the total global radiation measured at the Earth's surface divided by the extraterrestrial flux. To avoid contamination by surrounding objects, only the data corresponding to a solar zenith angle less than 70° were considered. For very small transmissivities (<0.05), which were caused by heavy convective clouds, $\Delta\alpha$ is negligible. For transmissivities greater than 0.5, $\Delta\alpha$ appears to be randomly scattered. However, for transmissivities greater than 0.05 and less than 0.5, α_S is greater than α_B. The largest differences in $\Delta\alpha$ are found when $T_s \sim 0.2$. These results indicate that under nonpolluted atmospheric conditions, clouds attenuate total radiation more than UV-B radiation. The variation of $\Delta\alpha$ as a function of transmissivity could imply that $\Delta\alpha$ is proportional to the cloud optical depth. There appears to be two physical phenomena occurring: one for trans-

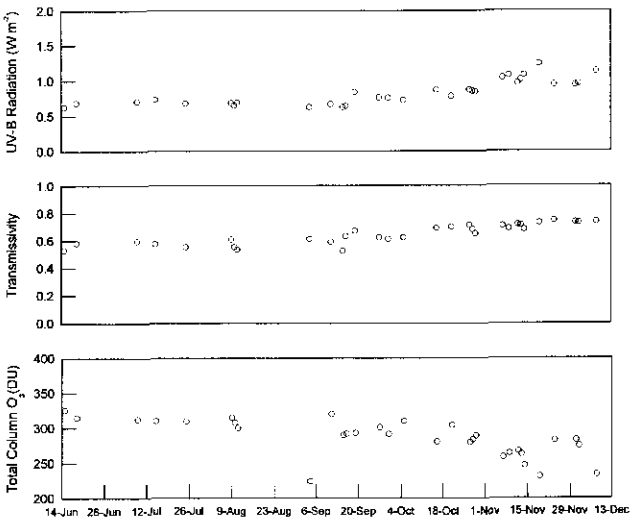

Figure 6. Scatter plot of UV-B radiation, total solar transmissivity, and total column O_3 for 31 clear sky mornings when the solar zenith angle was 60°. Note the increase in UV-B radiation and transmissivity and decrease in total column O_3 from summer to autumn.

missivities greater than 0.2 and the other when transmissivity is less than 0.2. The decrease in the total radiation attenuation (or the increase of total radiation reaching the surface in conjunction with a decrease in UV-B radiation at the surface) for transmissivities less than 0.2 could be explained by the fact that the albedo over cloud ice is twice the albedo over cloud water and that the albedo for the UV-B is greater than the albedo of total global radiation [*Kondratyev*, 1969]. This would produce

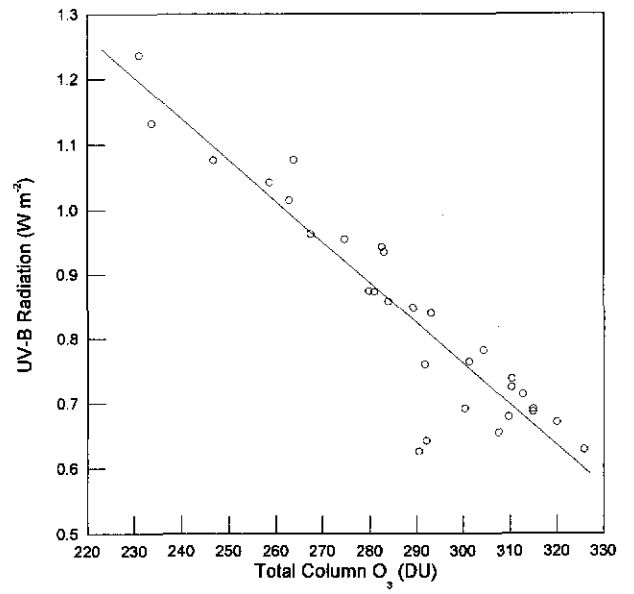

Figure 7. Scatter plot of UV-B radiation as a function of total column O_3 for 31 clear sky mornings when the solar zenith angle was 60°. Note the solid line is a linear regression fit. A decrease in ozone from 270 to 260 DU produces an increase of 6.2% in UV-B radiation, while a decrease in ozone from 330 DU to 220 DU produces an increase in UV-B radiation of 33%.

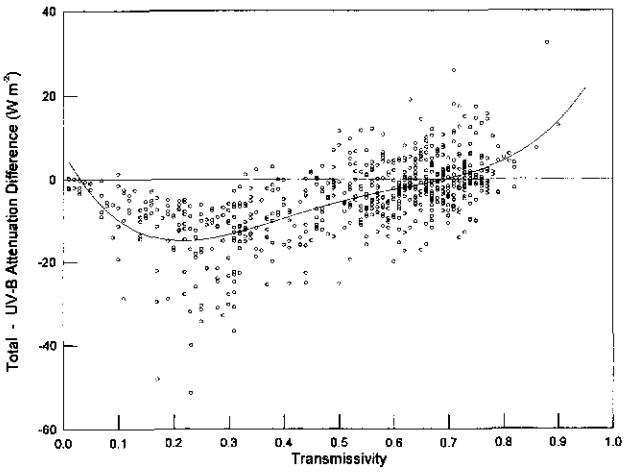

Figure 8. Difference between total solar and UV-B radiation attenuation as a function of total solar transmissivity from June 14 to August 31, 1994. Note the curve is a fourth-degree polynomial fit to show trend of the attenuation difference.

an increase in backscattered UV-B radiation to space from the ice cloud tops which will cause a decrease in the ratio of UV to total radiation when the transmissivity is less than 0.2. When the transmissivity is greater than 0.2, the ratio of UV to total radiation increases. This increase in the ratio is due to the fact that clouds produce an increase in scattering of UV-B radiation [*Ambach et al.*, 1991]. The result is an increase in the attenuation of total radiation. Clouds also absorb radiation more effectively in the near-infrared which means that the albedo of clouds is higher for visible and ultraviolet than for the near-infrared [*Kondratyev*, 1969]. Another possible explanation that could explain the attenuation of solar radiation is more that the attenuation of UV-B radiation may be due to an incomplete separation between ozone and aerosol effects.

Increases of UV-B Radiation Above Normal Clear Sky Values

An example of the increase in both transmissivity and UV-B radiation over the normal clear sky values is evident on July 31, 1994 (Figure 9). For a solar zenith angle of 17.7° the UV-B radiation reaching the surface was measured at 3.87 W m^{-2}. Fifteen minutes earlier, the NWS reported that 80% of the sky was covered by clouds, of which 30% were cumulus and the remaining 50% altocumulus. The observed UV-B radiation increase was 26.6% after correcting the measured clear sky UV-B radiation for variation in total column O_3. Simultaneous readings of global radiation also confirm the measured UV-B radiation increase. The measured global radiation was 1220 W m^{-2} which corresponded to a transmissivity of 0.95, higher than an expected value of 0.80 for clear skies and good visibility [*Gates*, 1980]. *Nack and Green* [1974] forecasted a possible increase of UV radiation up to 25% due to scattering by and transmission through clouds.

Table 4 summarizes all of the UV-B radiation increases greater than 20%. Upon examination of these data, it becomes apparent that nearly all of the UV-B increases occurred during the summer afternoons for relatively short periods of time (less than 10 min). For cases when the UV-B increases were less than 20%, the time span of these measured increases ranged between several minutes to 1 hour. The increases of UV-B

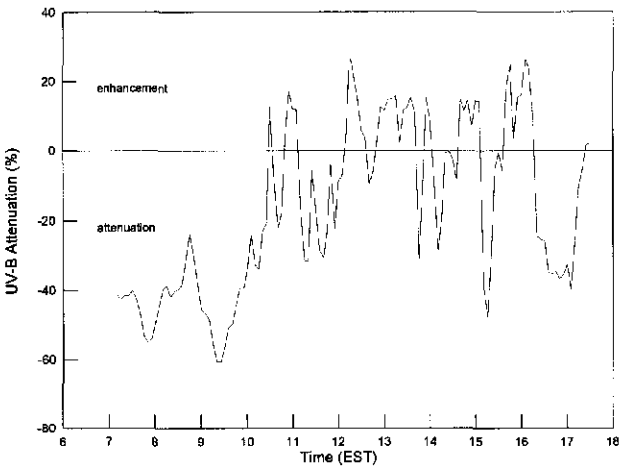

Figure 9. Time series of UV-B attenuation for July 31, 1994. Note the increases in UV-B radiation above clear sky levels from late morning through much of the afternoon.

radiation can be explained by the increase of clouds due to strong tropospheric convection. The average solar zenith angle for these cases was 53.5°. Two of the largest UV-B radiation increases were observed on July 20 (26.8%) and July 31 (26.6%) in which 90% and 80% of the sky was covered by clouds, respectively. Studies conducted by *Bais et al.* [1993] and *McCormick and Suehrcke* [1990] found that slight increases in UV-B radiation were observed above normal levels only for partly cloudy conditions. *Mims and Frederick* [1994] found peak increases of nearly 20% at the Mauna Loa Observatory in Hawaii. Although the data presented here suggests that cloud coverage of 80 to 90% may be the cause of the greatest local UV-B increases, more data are required to properly address this problem.

On several occasions, total and UV-B radiation values increased as cumulus clouds passed near the zenith with the rest of the sky free of clouds. It is important to note that the Sun was near its solar noon position, but the clouds never directly blocked the Sun itself. As these clouds moved away from the zenith, the total and UV-B radiation values returned to near normal readings. The timescale of these phenomena was generally on the order of several minutes. *Kondratyev* [1969] reports that the ratio of diffuse to direct total radiation was observed to increase from 1.6 to 6.8 due to an increase in cumulus clouds in the circumsolar region. It is possible that the passage of cumulus clouds near the Sun could explain the increases of UV-B radiation under partly cloudy conditions reported by *Bais et al.* [1993] and *McCormick and Suehrcke* [1990]. Different cloud morphologies and/or surface albedos could also explain this phenomena.

Observations from June 29 depict a case when a break in the clouds from an overcast sky allowed the direct radiation of the Sun to reach the surface. The NWS reported overcast stratocumulus clouds during most of the morning. The UV-B attenuation was 41% when the Sun was obstructed by clouds at an zenith angle of 50°. For a short period of time (~ 1 minute) when the Sun was visible through a break in the clouds, the UV-B radiation received at the surface was comparable to levels normally characterized by clear skies. Stratocumulus

Table 4. Summary of UV-B Increases Greater Than 20%

Date	Time, EST	Solar Zenith Angle, deg	Observed UV-B, W m^{-2}	Clear Sky UV-B, W m^{-2}	Increase of UV-B, Percent	T_s	Sky Conditions
June 24	0735	61.4	0.73	0.61	20.5	0.71	7, 3Cu20, 4AcE130
July 17	1645	58.6	1.01	0.83	22.4	0.80	9, 1Tcu50, 2Ac130, 6CsE200
	1650	59.6	0.95	0.78	22.2	0.78	9, 1Tcu50, 2Ac130, 6CsE200
	1655	60.6	0.88	0.73	21.3	0.79	9, 1Tcu50, 2Ac130, 6CsE200
July 20	1350	24.6	3.59	2.83	26.8	0.91	9, 1Cb10, 2Ac120, 5AsE150, 1Ci300
	1355	25.4	3.44	2.79	23.1	0.85	9, 1Cb10, 2Ac120, 5AsE150, 1Ci300
	1620	53.8	1.35	1.11	22.0	0.74	8, 5Tcu30, 2AcE120, 1Ci250
	1625	54.8	1.28	1.04	22.3	0.77	8, 5Tcu30, 2AcE120, 1Ci250
	1640	57.8	1.05	0.87	20.0	0.67	6, 3Tcu31, 1Ac120, 2CsE250
July 23	1655	61.1	0.89	0.70	22.8	0.78	8, 6TcuM35, 2Ci250
	1700	62.1	0.79	0.65	20.6	0.74	8, 6TcuM35, 2Ci250
July 29	1715	65.8	0.62	0.50	22.2	0.73	8, 0Cb30, 6TcuM35, 2Ci250
	1720	66.8	0.60	0.47	24.7	0.74	8, 0Cb30, 6TcuM35, 2Ci250
	1725	67.8	0.54	0.44	22.3	0.76	8, 0Cb30, 6TcuM35, 2Ci250
July 31	1215	17.7	3.87	3.05	26.6	0.95	8, 3Cu23, 5AcE120
	1220	17.6	3.75	3.05	22.5	0.90	8, 3Cu23, 5AcE120
	1545	47.9	1.84	1.47	24.8	0.85	9, 5Cb40, 2ScM60, 2Ac110, 0Ci250
	1605	51.9	1.52	1.21	26.2	0.78	9, 5Cb40, 2ScM60, 2Ac110, 0Ci250
	1610	52.9	1.41	1.14	23.0	0.75	9, 5Cb40, 2ScM60, 2Ac110, 0Ci250
August 1	1650	61.2	0.84	0.70	21.1	0.78	8, 6CbM63, 0Ac120, 2Ci250
	1655	62.2	0.79	0.65	21.1	0.73	8, 6CbM63, 0Ac120, 2Ci250
August 14	1545	50.4	1.64	1.33	22.4	0.75	6, 6CuM40, 0Ci250
	1550	51.4	1.55	1.27	22.1	0.80	6, 6CuM40, 0Ci250
	1610	55.4	1.26	1.02	23.5	0.73	6, 6CuM40, 0Ci250
	1615	56.4	1.18	0.96	22.1	0.68	6, 6CuM40, 0Ci250
	1625	58.4	1.06	0.85	24.9	0.74	6, 6CuM40, 0Ci250
	1630	59.4	0.96	0.80	20.4	0.66	6, 6CuM40, 0Ci250
	1650	63.5	0.75	0.61	23.7	0.69	5, 4Cu40, 1Ci250
	1655	64.5	0.68	0.57	20.1	0.63	5, 4Cu40, 1Ci250

type clouds apparently do not produce a measurable increase of UV-B radiation over the normal clear sky value. This probably is due to the fact that stratocumulus clouds lack the vertical dimensions that convective-type cumulus clouds have which act as reflectors of total and UV-B radiation.

The increase of UV-B radiation by clouds merits further study, especially considering the potential impact that this phenomenon can have on regions where deep convective clouds dominate. Maximum UV-B increases will be expected in regions where there is little haze and convective activity is significant. Global radiation values have been measured up to 1500 W m^{-2} at high elevations with scattered clouds [*Gates*, 1980]. It follows that localized increases of UV-B radiation are to be expected under similar conditions. It is important to note that these increases in UV-B radiation occur on very short timescales, usually on the order of minutes. Since these data were sampled at 1 Hz and averaged over 5-min intervals, then it is quite likely that high values of UV-B radiation have been averaged out. Future studies should attempt to gather data over shorter periods of time to better address this issue.

Summary

The effects of clouds and haze on UV-B attenuation have been investigated for a 6-month period in Research Triangle Park, North Carolina. An empirical relationship was derived to predict UV-B attenuation as a function of total solar transmissivity and cloud cover. This relationship has the advantage of including transmissivity which has not be used in previous studies. Local cloud position seems to be a critical factor in UV-B increases or decreases. Cumulus-type clouds have been found to attenuate UV-B radiation by as much as 99% when the solar disk was obscured. However, these same cloud types were also found to produce local increases in UV-B radiation due to scattering from the sides of those clouds. A maximum increase of nearly 27% was observed with 90% of the sky covered by clouds and the direct beam unobstructed. Summertime haze under clear skies attenuates UV-B radiation between 5% and 23% for a solar zenith angle of 34° compared to a clear sky day in the autumn. Total radiation fluxes were found to be reduced up to 24% more than the UV-B radiation fluxes due to clouds.

Acknowledgments. This research has been funded through a cooperative agreement (CR820074-01-0) between the National Exposure Research Laboratory of the U. S. Environmental Protection Agency and the Department of Marine, Earth, and Atmospheric Sciences of the North Carolina State University. Special thanks are extended to Jeff Jarvis and the RDU NWS staff for providing the meteorological data. The authors also wish to express their sincere appreciation to Sasha Madronich of the National Center for Atmospheric Research for providing the code to his radiative transfer model. Thanks also to Alan Huber for his comments and suggestions on this research. The authors also wish to thank Betsy Weatherhead, John DeLuisi, Craig Long, and Joe Pinto for their thoughtful reviews of this manuscript. This document has been reviewed in accordance with U. S. Environmental Protection Agency policy and approved for publication. Mention of trade names or commercial products does not constitute endorsement or recommendation for use.

References

Ambach, W., M. Blumthaler, and G. Wendler, A comparison of ultraviolet radiation measured at Arctic and an alpine site, *Solar Energ.*, *47*, 121–126, 1991.

Bais, A. F., C. S. Zerefos, C. Meleti, I. C. Ziomas, and C. Tourpali, Spectral measurements of solar UVB radiation and its relations to total ozone, SO_2, and clouds, *J. Geophys. Res.*, *98*, 5199–5208, 1993.

Blumthaler, M., and W. Ambach, Human solar ultraviolet radiant exposure in high mountains, *Atmos. Environ.*, *22*, 749–753, 1988.

Cutchis, P., A formula for comparing annual damaging ultraviolet (DUV) radiation doses at tropical and midlatitude sites, *Fed. Av. Admin. Rep. FAA-EE 80-81*, U. S. Dep. of Transp., Washington, D. C., 1980.

Dickerson, R. R., D. H. Stedman, and A. C. Delany, Direct measurements of ozone and nitrogen dioxide photolysis rates in the troposphere, *J. Geophys. Res.*, *87*, 4933–4946, 1982.

Frederick, J. E., and H. D. Steele, The transmission of sunlight through cloudy skies: an analysis based on standard meteorological information, *J. Appl. Meteorol.*, *34*, 2755–2761, 1995.

Frederick, J. E., E. K. Koob, A. D. Alberts, and E. C. Weatherhead, Empirical studies of tropospheric transmission in the ultraviolet: broadband measurements, *J. Appl. Meteorol.*, *32*, 1883–1892, 1993.

Gates, D. M., *Biophysical Ecology*, 601 pp., Springer-Verlag, New York, 1980.

Haurwitz, B., Insolation in relation to cloud type, *J. Meteorol.*, *5*, 110–113, 1948.

Ilyas, M., Effect of cloudiness on solar ultraviolet radiation reaching the surface, *Atmos. Environ.*, *21*, 1483–1484, 1987.

Iqbal, M., *An Introduction to Solar Radiation*, 390 pp., Academic, San Diego, Calif., 1983.

Josefsson, W., Solar ultraviolet radiation in Sweden, *SMHI Rep. 53*, Nat. Inst. of Radiat. Protect. in Stockholm, Norrköping, Sweden, 1986.

Justus, C. G., and B. B. Murphey, Temporal trends in surface irradiance at ultraviolet wavelengths, *J. Geophys. Res.*, *99*, 1389–1394, 1994.

Koller, L. R., *Ultraviolet Radiation*, 611 pp., John Wiley, New York, 1965.

Kondratyev, K. Y., *Radiation in the Atmosphere*, 912 pp., Academic, San Diego, Calif., 1969.

Liu, K. N., and N. P. Jordan, The interrelationship and characteristic distribution of direct, diffuse, and total solar energy, *Solar Energy*, *4*, 19, 1960.

Madronich, S., The atmosphere and UV-B radiation at ground level, in *Environmental UV Photobiology*, edited by A. R. Young, pp. 1–39, Plenum Press, New York, 1993.

McCormick, P. G., and H. Suehrcke, Cloud-reflected radiation, *Nature*, *345*, 773, 1990.

Miller, A. J., C. Long, and H. T. Lee, *Ultraviolet Potential Index*, NOAA/NWS/National Meteorological Center, Washington, D. C. and Research and Data Systems Corp., Greenbelt, Md., 1993.

Mims, F. M., III, and J. E. Frederick, Cumulus clouds and UV-B, *Nature*, 371, 291, 1994.

Molina, L. T., and M. J. Molina, Absolute absorption cross sections of ozone in the 185- to 350-nm wavelength range, *J. Geophys. Res.*, *91*, 14,501–14,508, 1986.

Nack, M. L., and A. E. S. Green, Influence of clouds, haze, and smog on the middle ultraviolet reaching the ground, *Applied Optics*, *13*, 2405–2415, 1974.

Page, S. H., National land use and land cover inventory, *U. S. EPA Tech. Note, EMSL-LV Project AMD 7974*, Environ. Protect. Agency, Las Vegas, Nev., 1980.

Paltridge, G. W., and I. J. Barton, Erythemal ultraviolet radiation distribution over Australia—the calculations, detailed results and input data including frequency analysis of observed Australian cloud cover, Commonwealth Scientific and Industrial Research Organization Technical Paper, *Div. Atmos. Phys. Techn. Pap. 33*, 1978.

Peak, M. J., J. G. Peak, M. P. Mohering, and R. B. Webb, Ultraviolet action spectra for DNA dimer induction, lethality and mutagenesis in Escherichia coli with emphasis on the UV-B region, *Photochem. Photobiol.*, *40*, 613–620, 1984.

Setlow, R. B., The wavelengths in sunlight effective in producing skin cancer: A theoretical analysis, *Proc. Natl. Acad. Sci.*, *71*, 3363–3366, 1974.

Spencer, J. W., Fourier series representation of the position of the sun, *Search*, *2*, 172, 1971.

Sullivan, J., Effects of UV-B radiation on terrestrial plants, Proceedings, UV-B Monitoring Workshop: A Review of the Science and Status of Measuring and Monitoring Programs, U. S. Department of Agriculture, Washington, D. C., March 10–12, 1992.

W. F. Barnard, Atmospheric Process Research Division, National Exposure Research Laboratory, USEPA, Research Triangle Park, NC 27111.

G. H. Crescenti and J. J. Streicher, Atmospheric Sciences Modeling Division, Air Resources Laboratory, NOAA, Research Triangle Park, NC 27111.

J. G. Estupiñán, Department of Geography, University of Colorado, Boulder, CO 80309.

S. Raman, Department of Marine, Earth, Atmospheric Sciences, North Carolina State University, Raleigh, NC 27695-8208.

(Received August 8, 1995; revised March 7, 1996;
accepted April 9, 1996.)